Preprints of the 19th World Congress
The International Federation of Automatic Control
Cape Town, South Africa. August 24-29, 2014

Experimentally Verified Depth Regulation for AUVs Using Constrained Model Predictive Control

Leo V Steenson * **Liuping Wang** ** **Alexander B Phillips** *
Stephen R Turnock * **Maaten E Furlong** *** **Eric Rogers** ****

* *Faculty of Engineering and the Environment, University of Southampton, Southampton SO17 1BJ, UK*
** *School of Electrical and Computer Engineering, RMIT University, Victoria, Australia*
*** *National Oceanography Centre (NOC), Southampton SO14 3ZH, UK*
**** *Electronics and Computer Science, University of Southampton, Southampton SO17 1BJ, UK (e-mail: etar@ecs.soton.ac.uk)*

Abstract: In the application of an autonomous underwater vehicle a critical requirement is to keep the level of the actuation signals within operational limits to avoid, for example, actuator nonlinearities and reduce peak power consumption. The most common approach to this problem for AUVs that have been deployed is, if required, to trade-off performance in order to keep the actuation signals and power required within the operational limits. This paper addresses depth control of an AUV using model predictive control with constraints on the both the amplitude and rate of change of the entries in the control vector. The model predictive control algorithm is designed by solving a quadratic programming problem in real-time when implemented on an AUV prototype. Experimental test results for depth control are also given and demonstrate that physically relevant constraints on the thrust and actuation power, critical factors for the use of these vehicles, can be achieved. Moreover, there is agreement between the control action used and the underlying physics of a body moving in water.

Keywords: Model predictive control, constrained design, AUVs

1. INTRODUCTION

Unmanned underwater vehicles (UUVs) are either remotely operated (ROVs) or autonomous (AUVs). The former are typically tethered to a ship or surface structure and the tether provides power and communication between the vehicle and operator. Use of a tether enables a pilot on the surface to manoeuvre the vehicle accurately and intelligently to complete a complex task, such as repairing an oil well riser. The major disadvantage of an ROV is that, due to the tether, the range of the vehicle is short and any motion of the ship is coupled with the vehicle itself.

AUVs are typically of torpedo shape, with four control surfaces and a propeller at the stern of the vehicle. These vehicles are used for long range survey type operations where the vehicle essentially acts like a bus for onboard sensors to log data, see, e.g., [McPhail, 2009]. Such missions include bathymetry, CTD (conductivity, temperature and depth), or mine detection surveys and many other survey-type missions. A typical AUV has an actuator set on-board and therefore there is a minimum speed below which the vehicle becomes unstable [Burcher and Rydill, 1994]. Such vehicles are therefore incapable of hovering and thus are unable to undertake detailed inspection-type missions.

The next generation of AUVs will require the ability to transit long distances, typical of standard AUVs, but also slow down to a hover in order to conduct inspections on areas of interest, typical of ROVs. To achieve this goal, a new approach is required to vehicle design and the on-board actuators. Moreover, implementation challenges to be solved include vehicle control using a multitude of actuators. In particular, there is an engineering supported need to impose magnitude and rate of change constraints on the control signals for more demanding missions, such as those arising in searching.

The dynamic model of an AUV system is nonlinear with multiple inputs and outputs. In addition, it is paramount to keep the level of the actuation signals within operational limits to, amongst others avoid actuator nonlinearities and reduce peak power consumption. Many previous control designs for AUVs do not place constraints on the control signals in the design and the result can be the need to detune the performance achieved in order to keep within the constraints (see, e.g., [Steenson et al., 2011a] and [Steenson et al., 2011b] for further discussion of this point from an end users viewpoint). The advances in Model Predictive Control (MPC) means that it is now feasible to consider design and experimental verification, and eventual deployment, of control laws designed with a

Fig. 1. Delphin2 AUV: Over-actuated hover capable AUV

priori constraints imposed on, e.g., the magnitudes of the control signals allowed.

This paper describes the design and implementation of an MPC scheme for depth control of AUVs, where operational constraints on the amplitudes and the rate of change of the control signals are imposed. The control signals are computed in real-time using a quadratic programming procedure. Supporting experimental results from an AUV are given where there is agreement between the control action used and the underlying physics of a body moving in water.

2. DELPHIN2 AUV AND DYNAMIC MODEL

The Delphin2 AUV shown in Fig. 1 is a prototype vehicle designed for the development and experimental verification of algorithms for control and navigation, where in this paper the former area is considered. This AUV is torpedo shaped and over-actuated with four through-body tunnel thrusters, four independently controlled control surfaces, and a rear propeller.

An AUV has a minimum velocity below which the vehicle becomes unstable. For the vehicle of Fig. 1 the through-body tunnel thrusters are used below this critical speed to maintain vehicle stability. Moreover, the thrusters are the dominant actuator set when operating between -0.3 ms^{-1} to 0.5 ms^{-1} forward speed.

To-date the Delphin2 AUV has used gain-scheduled Proportional plus Integral plus Derivative (PID) controllers for manoeuvring the vehicle, [Steenson et al., 2011a,b]. However, a number of factors, such as the use of a fixed value for the estimated buoyancy, could lead to poor/unacceptable performance when, e.g., performing complex manoeuvres or if the system unexpectedly changes due to loss or gain of buoyancy. Moreover, in operation there is an engineering need to place magnitude and rate constraints on the control signals for more demanding missions. Such constraints are not included in the PID design, leading to a control law that cannot be applied or degraded/unacceptbale performance. These reasons justify the use of designs, such as MPC, where such constraints can be imposed in the design stage.

The AUV can be modeled as two coupled second-order systems; depth and pitch, see Figure 2, and the equations of motion are

$$\begin{aligned}\dot{q}_v &= -\frac{1}{I_y}[x_{Tvf}T_{vf} + x_{Tvr}T_{vr} - z_g W\sin\theta \\ &\quad + \frac{1}{2}\rho V^{2/3} C_{Dq}|q_v|q_v], \\ q_v &= \int_0^t \dot{q}_v\ dt,\ \theta = \int_0^t q_v\ dt,\end{aligned} \tag{1}$$

for pitch and for depth

$$\begin{aligned}\dot{w}_v &= \frac{1}{m_z}[T_{vf}\cos\theta + T_{vr}\cos\theta + (W-B) \\ &\quad - \frac{1}{2}\rho V^{2/3} C_{Dw}|w_v|w_v], \\ w_v &= \int_0^t \dot{w}_v\ dt,\ z = \int_0^t w_v\ dt.\end{aligned} \tag{2}$$

The outputs from the controller are the force demands for each thruster (in Newtons (N)). To translate these force values into thruster speed set-points, that can be sent to the thruster controller, the inverse of the following thrust equation is used

$$n = 60 \times \left[\frac{T_{demand}}{\rho K_T D^4}\right]^{0.5}. \tag{3}$$

These equations calculate the angular acceleration about the y (pitch) axis and linear acceleration on the z (depth) axis respectively. The next step is to linearize them for MPC design. The various parameters in these motion equations are given in [Steenson, 2012] and only those used in the linear model approximation developed next are given in Table 1 below. Moreover, the damping terms will be described as quadratic, despite the inclusion of the absolute value (used to maintain correct sign).

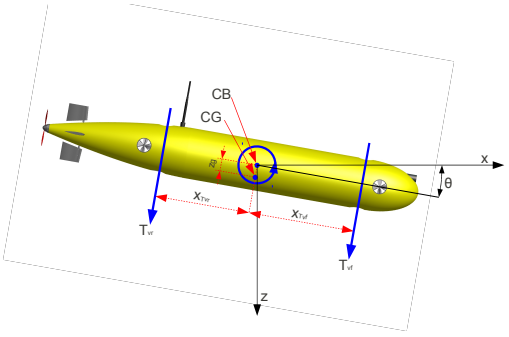

Fig. 2. Schematic of the location of the thruster force vectors, moment arms, center of gravity and buoyancy and the axis system, where the pitch angle is -10^o.

The trigonometric terms can be linearized by assuming small angles. Linearizing the quadratic damping terms is more challenging. When the AUV has successfully arrived at the defined depth and pitch set-points, and is stable, the heave and pitch velocities are zero and hence the damping forces and moments are equal to zero. Linearizing about zero heave and pitch velocities results in the damping coefficients also equalling zero, therefore eliminating damping from the model. Due to the

nonlinearities, removing damping from the model would force the MPC algorithm to reduce the system velocities using the system inputs (thrusters) rather than the natural dynamics, causing the controller to perform slowly and inefficiently. The linear damping terms therefore need to be a compromise between low and high speed operation and the resulting linearized state-space model for design is

$$\dot{x}(t) = \overbrace{\begin{bmatrix} 0 & 1 & 0 & 0 \\ 0 & \frac{\rho V^{2/3} k_z}{2m_z} & 0 & 0 \\ 0 & 0 & 0 & 1 \\ 0 & 0 & \frac{-z_g W}{I_y} & \frac{\rho V^{2/3} k_q}{2I_y} \end{bmatrix}}^{A} x(t) + \overbrace{\begin{bmatrix} 0 & 0 \\ \frac{1}{m_z} & \frac{1}{m_z} \\ 0 & 0 \\ \frac{-x_{Tvf}}{I_y} & \frac{-x_{Tvr}}{I_y} \end{bmatrix}}^{B} \begin{bmatrix} T_{vf} \\ T_{vr} \end{bmatrix}(t),$$

$$y(t) = \overbrace{\begin{bmatrix} 1 & 0 & 0 & 0 \\ 0 & 0 & 1 & 0 \end{bmatrix}}^{C} x(t), \tag{4}$$

where

$$x(t) = [\, z(t) \;\; w_v(t) \;\; \theta(t) \;\; q_v(t) \,]^T$$

and k_z and k_q are the linear damping coefficients. The values of the parameters used in this state-space model are given in Table 1 and for design and implementation the zero order hold sampling method is used with a sampling period of 0.1 secs.

Parameter	Value
ρ (*density*)	$1000 kg/m^3$
V (*velocity*)	$0.08 m^2$
m_z	$167.5 kg$
I_y (moment of inertia)	$70 kg.m^2$
W (weight)	$540 N$
k_z	8.62×10^{-2}
k_q	1.31×10^{-2}
x_{Tvf}	$0.55 m$
x_{Tvr}	-0.49

Table 1. Linear state-space model parameters.

As discussed earlier in this section, constraints on the magnitudes and rates of change of the control signals $T_{vf}(t)$ and $T_{vr}(t)$ in (4) are required. The rate of change of thrust demand should be chosen to be lower than the maximum rate that the thruster can change its speed (this is an approximation, as thrust is proportional to thruster speed squared). If the controller demands larger changes of thrust than the thruster is capable of producing, the thruster dynamics will effectively act as a low-pass filter, which may prove detrimental to controller performance when the control law is implemented experimentally. In this work the rate of change of set-points for each thruster are set at ± 2 N per sample.

The maximum absolute thrust value is set at +10 N, corresponding to a thruster speed of approximately 1800 rpm. The thrusters are capable of driving at higher speeds, and clearly producing more thrust, but it is desirable to reduce the peak thrust and thereby reduce peak electrical power consumption. The minimum absolute thrust value is set at +0.7 N, corresponding to a thruster speed of approximately 500 rpm. This is the minimum thruster speed below which the thruster dynamics become more non-linear due to the performance of the thruster controller (hardware) and the motor dead-band around zero thruster speed. Avoiding these non-linearities is the reason for setting the limit above zero speed.

3. MPC DESIGN

The first step in the MPC design is to discretize the continuous-time state-space model(4) to obtain

$$\begin{aligned} x_m(k+1) &= A_m x_m(k) + B_m u(k), \\ y(k) &= C_m x_m(k), \end{aligned} \tag{5}$$

where $A_m = e^{A_p h}$, $B_m = \int_0^h e^{A_p \tau} B_p d\tau$ and $C_m = C_p$; $x_m(k)$, $u(k)$ and $y(k)$ are the discrete state, input and output vectors respectively. The MPC algorithm used in this work [Wang, 2009] embeds an integrator into the model, enabling the controller to deal with model inaccuracies and ensure zero steady-state errors for set-point tracking. This is done by replacing the system state and input vectors by Δx and Δu, respectively, which are constructed by taking the difference between the current and previous state and input vectors, i.e.,

$$\begin{aligned} \Delta x_m(k) &= x_m(k) - x_m(k-1), \\ \Delta u(k) &= u(k) - u(k-1). \end{aligned} \tag{6}$$

Introducing

$$x(k) = \left[\Delta x_m(k)^T y^T(k)\right]^T, \tag{7}$$

gives the following state-space model for use in design

$$\begin{bmatrix} \Delta x_m(k+1) \\ y(k+1) \end{bmatrix} = \overbrace{\begin{bmatrix} A_m & 0 \\ C_m A_m & I \end{bmatrix}}^{\mathrm{A}} \begin{bmatrix} \Delta x_m(k) \\ y(k) \end{bmatrix} + \overbrace{\begin{bmatrix} B_m \\ C_m B_m \end{bmatrix}}^{\mathrm{B}} \Delta u(k) \tag{8}$$

$$y(k) = \overbrace{[0 \;\; I]}^{\mathrm{C}} \begin{bmatrix} \Delta x_m(k) \\ y(k) \end{bmatrix}, \tag{9}$$

where for the rest of the paper 0 and I denote the null matrices, respectively, with compatible dimensions.

In this model it is $\Delta u(k)$ that is optimized by the predictive control algorithm. In the steady-state, all entries in $\Delta x_m(k)$ are zero and the steady-state values of the output vector $y(k)$ will be taken as the set-point vector entries. Therefore, with the integrator embedded, the steady-state values are not required, leading to simplification at the implementation stage.

The MPC design uses the receding horizon control principle, where the future state vector is calculated over

a prediction horizon of N_p samples for a future control trajectory of N_c samples, where $N_c \leq N_p$. The prediction will be denoted as starting from sample number $k > 0$. Introduce the vectors

$$\Delta U = \left[\Delta u^T(k) \ \Delta u^T(k+1) \ \dots \ \Delta u^T(k+N_c-1) \right]^T \quad (10)$$

$$X(k) = \left[x^T(k+1|k) \ \dots \ x^T(k+N_p|k) \right]^T. \quad (11)$$

where the notation $x(j+i|k$ denotes the value of $x(j+i)$ given $x(k)$. Then the state space model (8) can be used to recursively compute the future state vectors and output vectors, or in a more compact form,

$$Y = Fx(k) + \Phi \Delta U, \quad (12)$$

where

$$F = \begin{bmatrix} CA \\ CA^2 \\ CA^3 \\ \vdots \\ CA^{N_p} \end{bmatrix}, \quad (13)$$

$$\Phi = \begin{bmatrix} CB & 0 & 0 & ... & 0 \\ CAB & CB & 0 & ... & 0 \\ CA^2B & CAB & CB & ... & 0 \\ \vdots & & & & \\ CA^{N_p-1}B & CA^{N_p-2}B & CA^{N_p-3}B & ... & CA^{N_p-N_c}B \end{bmatrix}$$

and

$$Y = \left[y^T(k+1 \mid k) \ \dots \ y^T(k+N_p \mid k) \right]^T$$

For a given reference , or set-point, vector $r(k)$ at sample time k, the objective of the MPC under the receding horizon principle is to bring the predicted output as close as possible to this vector, where the entries in the set-point vector are assumed to remain constant in the optimization window. This objective is then translated into a design to find the control vector ΔU such that an error function between the set-point and the predicted output vectors is minimized.

The cost function used in this paper is

$$J = (R_s - Y)^T (R_s - Y) + \Delta U^T \bar{R} \Delta U, \quad (14)$$

where

$$R_s^T = \overbrace{\left[1 \ 1 \ \dots \ 1 \right]}^{N_p} r(k)$$

and routine analysis gives the optimal solution in the absence of constraints as

$$\Delta U = (\Phi^T \Phi + \bar{R})^{-1} \Phi^T (R_s - Fx(k)), \quad (15)$$

with the assumption that $(\Phi^T \Phi + \bar{R})^{-1}$ exists.

Using receding horizon control, only $\Delta u(k)$, a sub-vector of ΔU, is applied and the actual control vector applied to the plant is computed using

$$u(k) = u(k-1) + \Delta u(k) \quad (16)$$

where both the current optimal control $\Delta u(k)$ and the past value $u(k-1)$ are used. Since the current and past control vectors have the same steady-state value, if the first sample of the control vector is taken as the actual plant input before the closed-loop controller is activated, the computation of the control vector using (16) leads to the actual control vector for direct implementation. Hence the control vector has included its steady-state value, which is also part of the simplification in the MPC implementation.

As discussed in the previous section, there is an engineering need to place amplitude and rate constraints on the control vectors used. This is achieved by minimizing the cost function J of (14) in real-time with constraints imposed. Control amplitude constraints for the state-space model at sampling instant k are imposed in the form

$$u^{min} \leq u(k) \leq u^{max}, \quad (17)$$

where the entries in u^{min} and u^{max} are the lower and upper limits on the amplitude of the corresponding entry in the control vector. allowed. In this work the same values are imposed on each entry in the control vector, i.e., 0.7 N for the minimum and 10 N for the maximum, but this setting also allows for different values for each entry.

The constraints on $\Delta u(k) = u(k) - u(k-1)$ are

$$\Delta u^{min} \leq \Delta u(k) \leq \Delta u^{max} \quad (18)$$

where the entries in Δu^{min} and Δu^{max} correspond to the minimum and maximum allowable changes in the thruster set-points, respectively.

The MPC design is obtained by minimizing the cost function (14) subject to (17) and (18) by direct application of quadratic programming algorithms in, for example, [Wang, 2009] and the relevant references cited in this text. In this application, implementation of the control law requires direct measurement of all entries in $\left[\Delta x_m^T(k) \ y^T(k) \right]^T$ at each sampling instant k. The difficulty is that the state vector component $\Delta x_m(k)$ is not measurable but could be approximated as $\Delta x_m(k) = x_m(k) - x_m(k-1)$. If, however, there is a significant amount of noise corruption in $x_m(k)$, the computed difference $\Delta x_m(k)$ will amplify its effects. Hence an observer is used to estimate $\Delta x_m(k)$ as

$$\hat{x}(k+1) = A\hat{x}(k) + B\Delta u(k) + K_{ob}(y(k) - C\hat{x}(k)) \quad (19)$$

where the observer gain matrix K_{ob} is chosen such that the closed-loop observer error system matrix $A - K_{ob}C$ has all eigenvalues strictly inside the unit circle of the complex plane. In this paper K_{ob} is designed using discrete-linear quadratic regulator theory with weighting matrices Q_{ob} and R_{ob}. If $R_{ob} = r_{ob}I$, the effects of measurement noise in $y(k)$ can be reduced by selecting a large value of r_{ob}. The initial state vector of the observer is taken as the zero vector if the output vector $y(k)$ is zero. Otherwise, the initial $\hat{\Delta} x_m(0)$ is set to zero and the initial $\hat{y}(0)$ is set to the actual measurement of $y(0)$.

4. EXPERIMENTAL VERIFICATION

Prior to the experimental tests, an in-depth simulation exercise was undertaken. These simulations were performed in MATLAB using the non-linear model of the system where realistic levels of measurement noise were added to the depth and pitch feedback signals. From the simulation results, given in [Steenson, 2012], three controller parameter sets were found corresponding to an aggressive, conservative and balanced system response, see Table 4.

The simulation studies were also used to determine the observer gain matrix by examining the effect of the observer gain scalar, r_o, on system performance. Although system performance does vary with r_o, it did not show any instability despite a wide range of values tested. For the experimental results given in the rest of this section $r_o = 50$ was used.

Controller set	N_p	N_c	r_w
Aggressive	60	8	0.5
Balanced	80	8	4.0
Conservative	100	8	8.0

Table 2. MPC design parameters for the experimental tests.

Figure 3 gives the simulation results when the AUV is diving from 0 to 1 depth whilst maintaining a zero pitch angle. The depth converges quickly with minimal overshoot but the pitch does oscillate slightly about zero degrees.

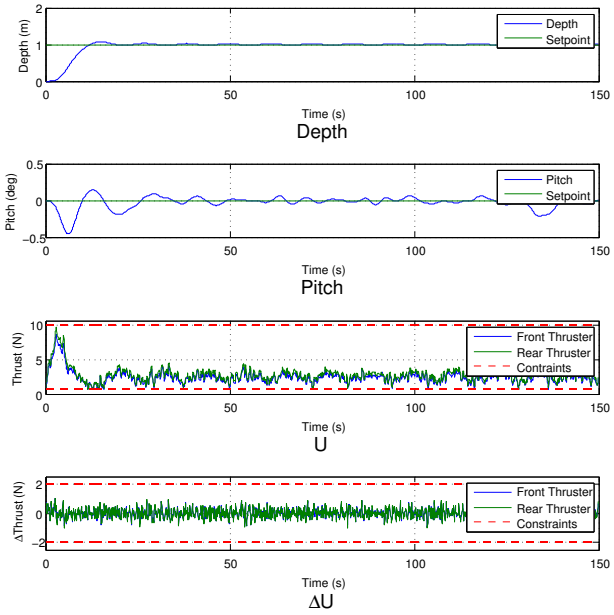

Fig. 3. Simulation results for the MPC controller using the observer with $r_o = 10$. The noise still effects the controller performance but within acceptable limits.

To test the MPC controller on the Delphin2 AUV, the MATLAB code was translated into the Python programming language and then integrated into the vehicles control software.

The experimental results were obtained in an acoustic tank measuring $8.0 \times 8.0 \times 4$ m deep. Each test consists of three depth set-points of 1.0 m, 3.0 m and 2.0 m with the pitch set-point set at 0.0^o for all the tests. Once the AUV has stayed within ± 0.2 m of the depth set-point for 60 secs it moves on to the next depth set-point.

Figures 4, 5 and 6, respectively, show the experimental results for the aggressive, balanced and conservative tuning parameter sets of Table 4, where the depth and pitch, u and Δu, signals are plotted against time.

These experimental results provide very strong evidence that the MPC with constraints algorithm is capable of high quality performance in this application area, where all three controller parameter sets provide stable control of both depth and pitch. Figure 4 confirms that the maximum thrust operational constraint of 10 N is only activated during the maximum velocity phases of descending operations, when the thrust is required to overcome both the positive buoyancy of the vehicle and the fluid drag due to the vehicle descending. This maximum thrust operation

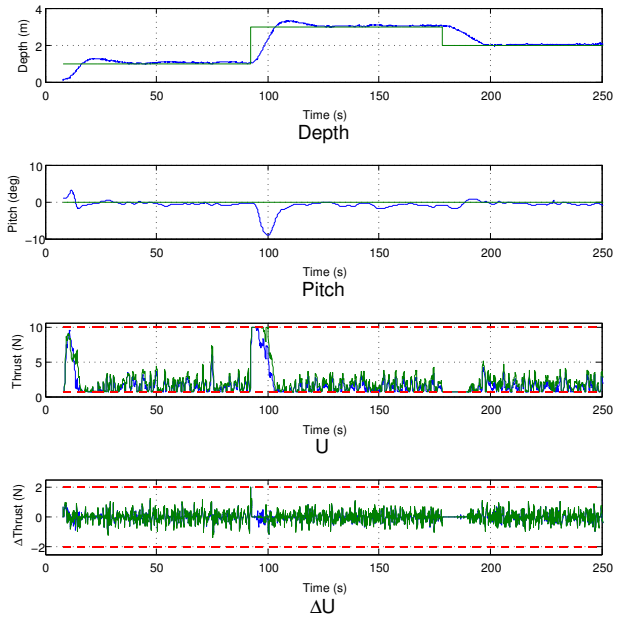

Fig. 4. Experimental results for the MPC controller with depth set-points of 1 m, 3 m and 2 m. The pitch set-point remains fixed at 0.0^o. Controller parameters: $Np = 60$, $Nc = 8$, $r_w = 0.5$, $r_o = 50$.

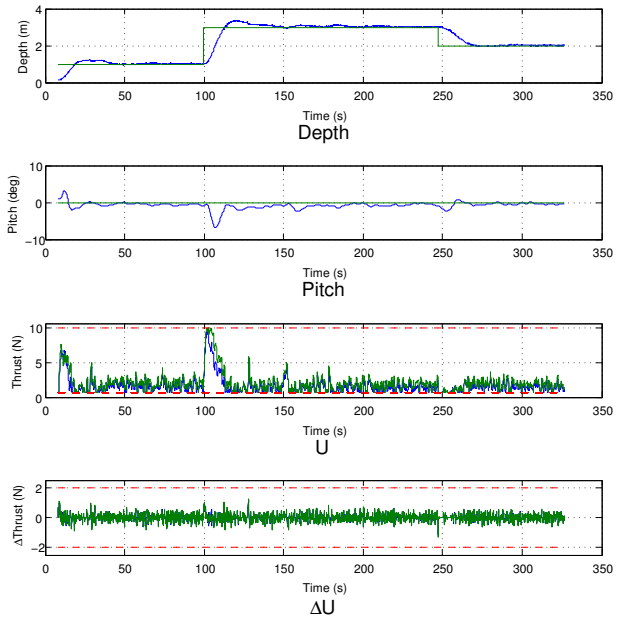

Fig. 5. Experimental results for the MPC controller with depth set-points of 1 m, 3 m and 2 m. The pitch set-point remains fixed at 0.0^o. Controller parameters: $Np = 80$, $Nc = 8$, $r_w = 4.0$, $r_o = 50$.

corresponds to the maximum actuation power. Moreover, the minimum thrust constraint of 0 N is activated during ascending operations, where the vehicle rises due to its positive buoyancy and thus no actuation power is required. Further application specific conclusions from these experimental results are given next, starting with the overshoot of the depth demand for all three parameter sets.

The overshoots for these parameter sets result in lower overshoot values for the larger values r_w with a minimum overshoot of 0.15 m with $r_w = 8$. This means that at the

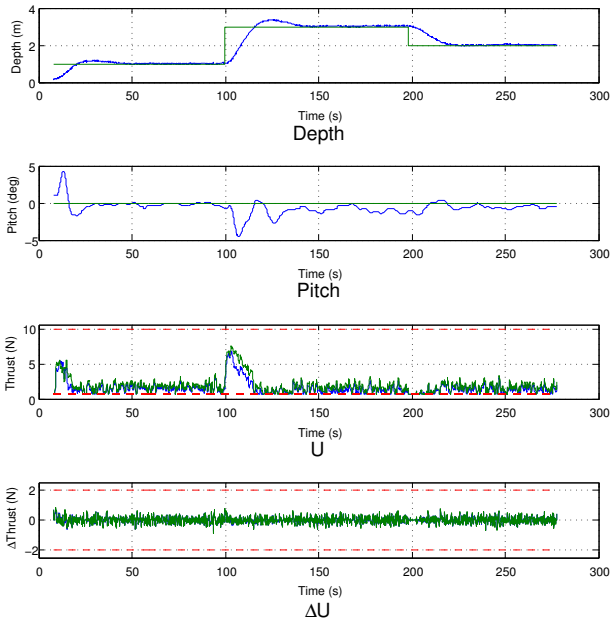

Fig. 6. Experimental results for the MPC controller with depth set-points of 1 m, 3 m and 2 m. The pitch set-point remains fixed at 0.0^o. Controller parameters: $Np = 100$, $Nc = 8$, $r_w = 12.0$, $r_o = 50$.

first depth demand the more conservative MPC provides less overshoot. For the second depth demand of 3.0 m this trend is reversed, with the largest overshoot of 0.382 m for $r_w = 8$. The cause of this reversal in trend is due to the magnitude of the step change in depth demand, where the lower r_w values cause the system to behave more aggressively with rapid changes in the entries in u, whilst the higher N_p values along with higher r_w values cause the controller to perform more conservatively.

For the first step change of 1.0 m, the more aggressive controller with a r_w value of 0.5 together with an N_p value of 60 causes the system to accelerate quickly, resulting in a large heave velocity which in turn results in it overshooting the depth demand. In contrast the more conservative controller parameters do not generate high heave velocities and hence corresponding overshoots are lower. This variation in controller 'aggressiveness' leads to the reversal in overshoot trends when the depth step change is greater. In this case all the controller parameters cause high heave velocities, but as the vehicle approaches the depth set-point the conservative controller parameters are slower to reduce the thrust magnitude and so their heave velocities decrease slower than the more aggressive controller parameters resulting in a greater overshoot. Further work on tuning the design in response to these first experimental results could be beneficial.

For the second step change, the constraints on the magnitude of thruster movement and its incremental movement have become active, i.e., used the maximum u and Δu, when the aggressive MPC is used, see Figure 4. As a result, the settling time is about 25 secs, which is about half of the response time in comparison with the cases when the balanced and conservative predictive controllers are used, see Figures 5 and 6). Hence, by deploying constrained control, the AUV system can provide the fastest response to the depth set-point signal while maintaining all operational constraints.

5. CONCLUSIONS

The contributions in this paper are on the application of MPC with magnitude and rate constraints on the control signals motivated by requirements for next generation AUVs. Experimental results demonstrate that by using a constrained control design, the response to depth set-point signals is significantly reduced. The design has been supported by experimental results that confirm that the constraints are activated and the results obtained agree with the physics of a body moving in water. These results also suggest much further research to fully determine the potential of MPC in this area. For example, further work on tuning the design, in light of the discussion at the end of the previous section, is required. Also the disturbance rejection capabilities need to be investigated. Detailed comparisons with alternative designs are also required together with extensions to other modes of operation, including transiting long distances and this last mode of operation followed by hover.

REFERENCES

R. Burcher and L. Rydill. *Concepts in submarine design.* Cambridge Ocean Technology Series, 1994.

S. McPhail. Autosub6000: A deep diving long range auv. *Journal of Bionic Engineering*, 6:55–62, 2009.

L. V. Steenson. *Agile Underwater Robots for Long Range Ocean Exploration.* PhD thesis, University of Southampton, 2012.

L.V. Steenson, A.B. Phillips, E. Rogers, M.E. Furlong, and S.R. Turnock. Preliminary results of a hover capable auv attempting transitional flight. In *Unmanned Untethered Submersible Technology (UUST)*, 2011a.

L.V. Steenson, A.B. Phillips, E. Rogers, M.E. Furlong, and S.R. Turnock. Control of an auv from thruster actuated hover to control surface actuated flight. In *Specialists Meeting AVT-189/RSM-028, Assessment of Stability and Control Prediction, Methods for NATO Air & Sea Vehicles*, October 2011b.

L. Wang. *Model Predictive Control System Design and Implementation Using MATLAB.* Springer, Advances in Industrial Control Series, 2009.